ORIGINAL RESEARCH

Left Ventricular Torsion Shear Angle Volume Approach for Noninvasive Evaluation of Diastolic Dysfunction in Preserved Ejection Fraction

Oleg F. Sharifov, MD, PhD; Chun G. Schiros, PhD; Inmaculada Aban, PhD; Gilbert J. Perry, MD; Louis J. Dell'italia, MD; Steven G. Lloyd, MD, PhD; Thomas S. Denney Jr, PhD; Himanshu Gupta, MD, FACC

***Background*—**Accurate noninvasive diagnostic tools for evaluating left ventricular (LV) diastolic dysfunction (LVDD) are limited in preserved LV ejection fraction. We previously proposed the relationship of normalized rate of change in LV torsion shear angle (φ') to corresponding rate of change in LV volume (V') during early diastole (represented as $-d\varphi'/dV'$) as a measure of LV diastolic function. We prospectively evaluated diagnostic accuracy of $-d\varphi'/dV'$ in respect to invasive LV parameters.

***Methods and Results*—**Participants (n=36, age 61±7 years) with LV ejection fraction ≥50% and no acute myocardial infarction undergoing coronary angiography for chest pain and/or dyspnea evaluation were studied. High-fidelity invasive LV pressure measurements and cardiac magnetic resonance imaging with tissue tagging were performed. τ, the time constant of LV diastolic relaxation, was 58±10 milliseconds (mean±SD), and LV end-diastolic pressure was 14.5±5.5 mm Hg. Cardiac magnetic resonance imaging-derived $-d\varphi'/dV'$ was 5.6±3.7. The value of $-d\varphi'/dV'$ correlated with both τ and LV end-diastolic pressure (r=0.39 and 0.36, respectively, P<0.05). LVDD was defined as τ>48 milliseconds and LV end-diastolic pressure >12 mm Hg (LVDD1), or, alternatively, τ>48 milliseconds and LV end-diastolic pressure >16 mm Hg (LVDD2). Area under the curve (AUC) of $-d\varphi'/dV'$ for identifying LVDD1 was 0.83 (0.67-0.98, P=0.001), with sensitivity/specificity of 72%/100% for $-d\varphi'/dV' \geq 6.2$. AUC of $-d\varphi'/dV'$ for identifying LVDD_2 was 0.82 (0.64-1.00, P=0.006), with sensitivity/specificity of 76%/85% for $-d\varphi'/dV' \geq 6.9$. There were good limits of agreement between pre- and post-nitroglycerin $-d\varphi'/dV'$.

***Conclusions*—**The $-d\varphi'/dV'$ obtained from the LV torsion volume loop is a promising parameter for assessing global LVDD with preserved LV ejection fraction and requires further evaluation. **(*J Am Heart Assoc*. 2018;7:e007039. DOI: 10.1161/JAHA.117.007039.)**

Key Words: cardiac magnetic resonance imaging • diagnostic method • left ventricular diastolic dysfunction • left ventricular torsion shear angle • torsion

Left ventricular (LV) diastolic dysfunction (DD) is a major cause of heart failure.[1] Invasive parameters of LV end diastolic pressure (LVEDP) and time constant of relaxation (τ) provide reliable assessment of LVDD;[2] however, their routine use is limited due to procedural risks and high cost. Accurate noninvasive assessment of LVDD is highly desirable. Echocardiography is frequently used for such noninvasive assessment. A number of echocardiographic parameters have been proposed for assessing LVDD.[2,3] The diagnostic accuracy of commonly used echocardiographic parameters is limited in preserved LV ejection fraction (LVEF).[3-5] Recent 2016 American Society of Echocardiography guidelines have proposed an integrated approach for assessing LVDD.[3] This approach is based on a consensus statement and has not been validated in prospective studies.

Torsion is an important spatial characteristic of LV mechanical function.[6] The cardiac magnetic resonance (CMR) myocardial tissue-tagging technique allows for comprehensive assessment of LV myocardial strains and torsion.[7] Torsion results from the helical fiber arrangement of LV.[8] LV torsion from base to apex along a longitudinal axis is labelled

From the Departments of Medicine (O.F.S., C.G.S., G.J.P., L.J.D., S.G.L., H.G.) and Biostatistics (I.A.), University of Alabama at Birmingham, AL; VA Medical Center, Birmingham, AL (G.J.P., L.J.D., S.G.L., H.G.); Department of Electrical and Computer Engineering, Auburn University, Auburn, AL (T.S.D.); Cardiovascular Associates of the Southeast, Birmingham, AL (H.G.).

Accompanying Figures S1 through S6 are available at http://jaha.ahajournals.org/content/7/1/e007039/DC1/embed/inline-supplementary-material-1.pdf

Correspondence to: Himanshu Gupta, MD, FACC, 3980 Colonnade Parkway, Birmingham, AL 35243. E-mail: hgupta@cvapc.com

Received June 26, 2017; accepted October 30, 2017.

Clinical Perspective

What Is New?

- We demonstrate that the normalized rate of change of left ventricular (LV) torsion shear angle to the corresponding rate of change in LV volume during early diastole correlates with LV end-diastolic pressure and LV diastolic relaxation rate in participants with preserved ejection fraction.
- High diagnostic value is shown for this parameter to identify LV diastolic hemodynamic abnormalities in participants with preserved ejection fraction.

What Are the Clinical Implications?

- We have demonstrated a novel method using tagged cardiac magnetic resonance imaging that reliably estimates elevated LV filling pressure and abnormal LV relaxation and therefore can be useful to evaluate LV diastolic dysfunction with preserved ejection fraction.
- After prospective validation in evaluation of LV diastolic dysfunction, our proposed method may be extended to echocardiography.

as LV twist.[8] LV twist is preserved or augmented in patients with diastolic dysfunction and normal systolic performance.[8] LV torsion shear angle (φ) is twist normalized to long-axis length and LV radius.[9] We previously proposed a novel CMR approach to assess LVDD; it utilizes normalized LV torsion shear angle volume (normalized φ is indicated as φ', and normalized LV volume is indicated as V').[10] We found that the ratio of φ' change to increase in V' during early diastolic phase ($-d\varphi'/dV'$) was significantly increased in the hypertensive cohort, indicating reduced LV filling to the same changes of untwist when compared with the control cohort.[10] Here we sought to evaluate the relationship of CMR-obtained $-d\varphi'/dV'$ index to high-fidelity invasively measured markers of LV diastolic function in clinically stable patients with preserved LVEF and assess diagnostic accuracy in identifying invasively proved LVDD.

Methods

The data, analytic methods, and study materials will not be made available to other researchers for purposes of reproducing the results or replicating the procedure. Participants with chest pain and/or dyspnea undergoing diagnostic coronary angiography with preserved LVEF for evaluation of coronary artery disease (CAD) were prospectively enrolled between 2011 and 2015 (Figure 1). Major exclusion criteria included echocardiographic LVEF <50%, evidence of recent myocardial infarction, primary coronary intervention during cardiac catheterization, presence of hypertrophic cardiomyopathy, myocarditis, or significant valve disease, presence of

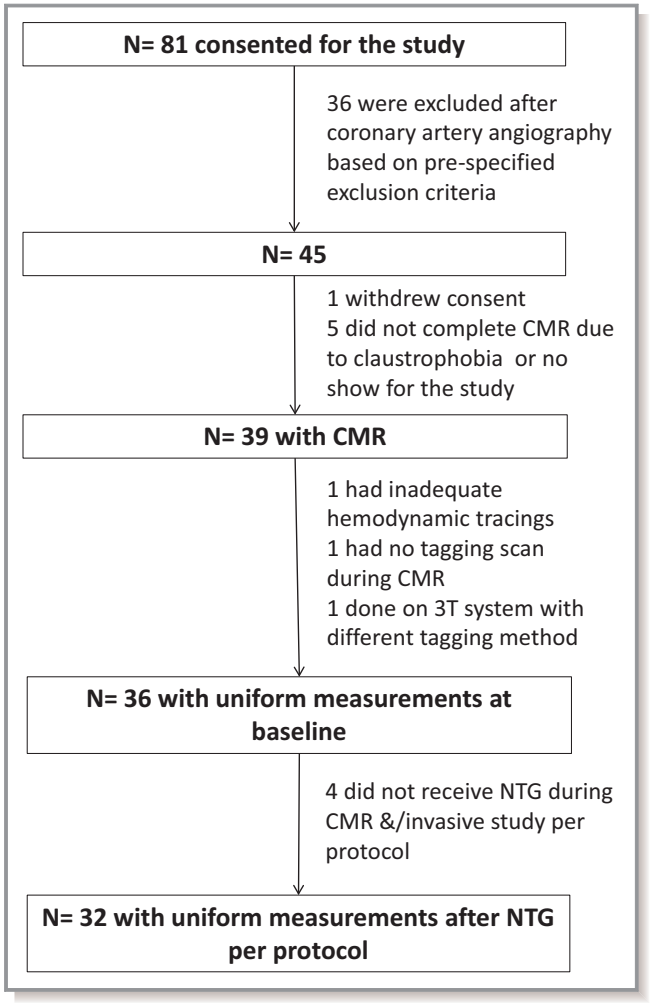

Figure 1. Study participant flow diagram. CMR indicates cardiovascular magnetic resonance imaging; NTG, nitroglycerin.

pacemaker or defibrillator or contraindication to cardiac magnetic resonance imaging. Figure 1 describes the flow of study participants. From 81 participants who consented for the study, only 36 met inclusion criteria and completed the study protocols required for uniform data analysis/presentation in this article (Figure 1). The study was approved by the University of Alabama at Birmingham and US Department of Veterans Affairs Institutional Review Board. All participants gave written informed consent.

LV Catheterization

Comprehensive hemodynamic assessment was performed using a high-fidelity manometer (Millar Instruments, Houston, TX, or St. Jude, Little Canada, MN). Multiple LV pressure tracings were acquired at baseline followed by sublingual nitroglycerin (NTG). LVEDP and minimum LV pressure were quantified from the median measurement obtained from 5 to 7 tracings with a total of ≈25 to 30 beats in a core laboratory

in a blinded fashion. Time constant of LV relaxation (τ) was assessed by the Weiss method,[11] which assumes that LV pressure decays monoexponentially (ME) to a 0 asymptote (τ-ME). For robustness, τ from the hybrid-logistic model of LV relaxation (τ-HL) and pressure half-time ($T_{½}$), defined as the time required for LV pressure at dP/dT_{min} to decline 50%, were also calculated.[12]

Cardiac Magnetic Resonance Imaging

Cine CMR was performed on a 1.5-T CMR scanner (Signa, GE Healthcare, Milwaukee, WI) optimized for cardiac imaging. Most of the studies were completed on the same day or the next 3 days (median 2 days) after cardiac catheterization. ECG-gated breath-hold steady-state free precision technique was used to obtain serial parallel short-axis LV views and long-axis views prescribed in circular orientation at 30° interval to allow for comprehensive LV coverage. The CMR parameters were slice thickness of the imaging planes 8 mm with 0 interslice gap, field of view 40 cm, scan matrix 256×128, flip angle 45°, repetition/echo times 3.8/1.6 milliseconds, and number of reconstructed cardiac phases 20. Tagged CMR was done at baseline and post-NTG on exact slice prescriptions as above by applying grid tagging to the short-axis views and stripe tagging to long-axis views using spatial modulation of magnetization encoding gradients method as previously described[10,13] with the following parameters: prospective ECG triggering, repetition/echo times 8.0/4.2 milliseconds, views per segment 8 to 10, tag spacing 7 mm, and number of reconstructed cardiac phases 20. Because the tag lines faded with time due to T1 relaxation, tagged image-derived parameters were valid only throughout systole and the first 67% of diastole.

LV geometric parameters were measured from endocardial and epicardial contours manually traced on cine images acquired near end-diastole and propagated throughout the cardiac cycle using in-house software.[14] LV and left atrial volumetric index calculation was computed as previously described.[15,16] LVED stress was calculated as previously described.[7]

Two-dimensional (2D) strain at each timeframe and rates were measured using harmonic phase analysis.[17] 2D apical and basal rotations at each timeframe were measured by tracking a circular mesh of points in the apical and basal slices of that timeframe. The mesh was identified in the first time-based on user-defined contours and tracked through the remaining imaged phases using improved harmonic phase tracking.[18] The 2D twist at timeframe t, T(t), was computed as the apical rotation minus the basal rotation at the same timeframe (Figure 2A). Twist time curve was constructed and differentiated to obtain the twist rate time curve. Peak twist rate and peak diastolic untwist rate were measured.[10] Peak twist per length at end systole and peak untwist per length rate were then calculated by dividing the peak end-systolic twist and peak untwist by the distance between the apical and basal slices at end diastole.[9,19] Torsion shear angle φ(t) at timeframe t was computed as[9,20]:

$$\varphi(t) = T(t) \times \frac{\rho_{base}(t) + \rho_{apex}(t)}{2L}$$

where ρ(t) is the epicardial radius at time t and L is the distance between the basal and distal slices at the end-diastole timeframe (Figure 2A). LV volume at timeframe t was computed using the previously described technique (Figure 2B and 2D).[14] A 2D φ(t) curve was therefore constructed for each subject (Figure 2C and 2E). For each subject, the φ(t) curve was normalized by its maximum to generate a φ′(t) curve, and the V(t) curve was normalized by its maximum to generate a V′(t) curve. The φ′(t) and V′(t) curves were then interpolated onto a common time so that end diastole and end systole occurred at the same point on both curves. The negative peak slope of the diastolic φ′ versus V′ curve (ie, $-d\varphi'/dV'$) was calculated as the slope of a linear regression model fit to the first 4 points of the diastolic φ′ versus V′ curve (Figure 2F).[10]

Two additional approaches were utilized to verify the robustness of our calculations. In the first approach ($-d\varphi'/dV'$ 2-point method), $-d\varphi'/dV'$ was calculated using a 2-point interval method when torsion difference was divided by the volume difference. In the second approach, LV twist was computed from tagged CMR using Fourier analysis of stimulated echoes (FAST), which determined object rotation in Fourier space in a basal and apical short-axis slice.[21] The basal was the most basal slice in which the LV myocardium maintained a continuous annular shape during the entire cardiac cycle. The apical slice was the most apical slice containing the presence of the blood pool throughout the entire cardiac cycle. FAST-computed LV twist was further used for $-d\varphi'/dV'$ (ie, $-d\varphi'/dV'$ FAST) calculation as described above.

Hemodynamic Indices for Abnormal LVEDP, τ-ME, and LVDD

On invasive hemodynamic measurements, LVEDP >12 mm Hg and τ-ME >48 milliseconds were considered abnormal.[2,22] LVDD was considered proven if both τ-ME and LVEDP were abnormal. All other participants with either prolonged τ-ME or elevated LVEDP or those without distinct hemodynamic abnormalities were considered as having marginal diastolic dysfunction and combined for analysis as "others." In secondary analysis we also evaluated an alternative LVEDP threshold of >16 mm Hg for diagnosing LVDD, defined as LVEDP >16 mm Hg and τ-ME >48 milliseconds.[2]

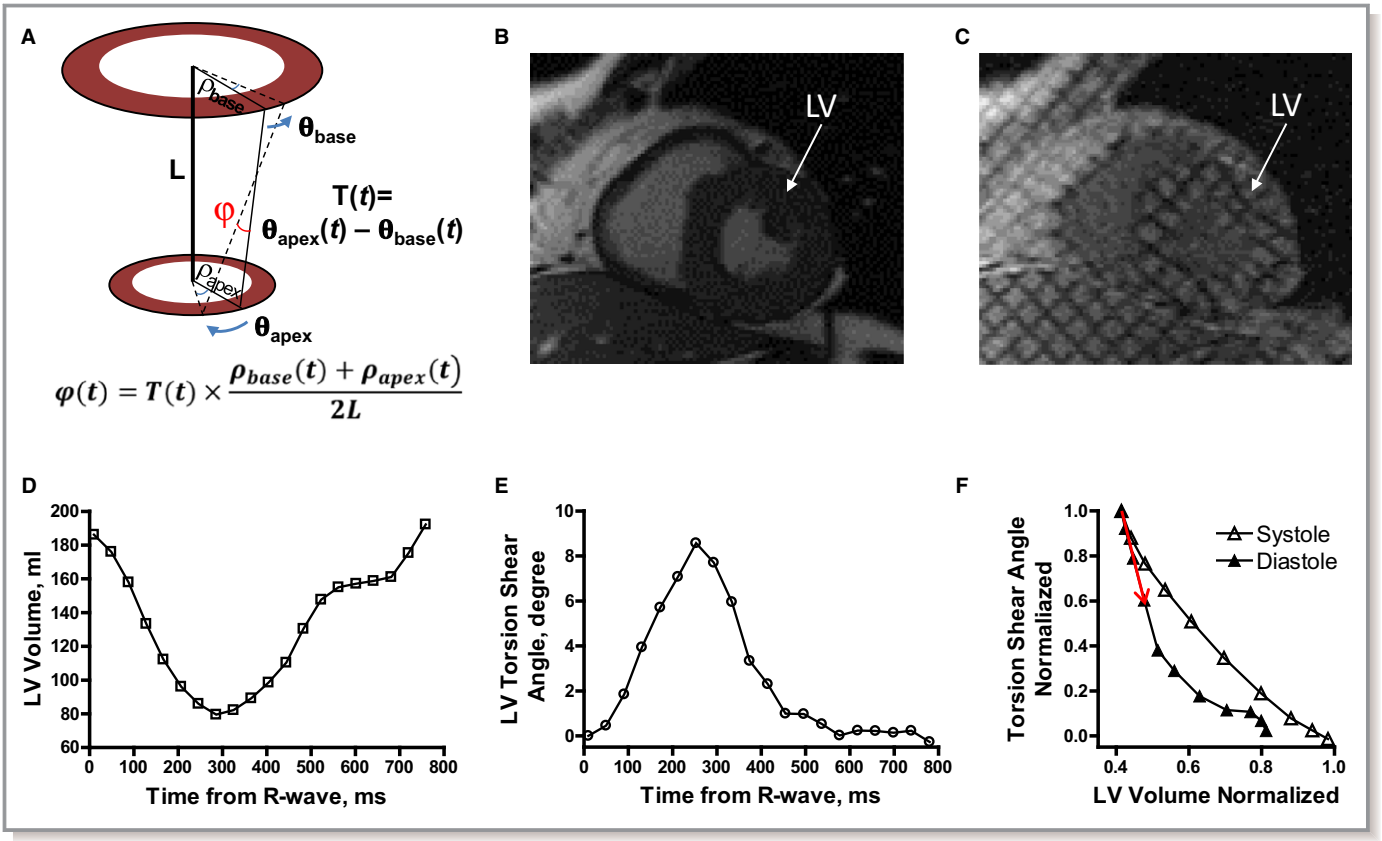

Figure 2. Methodology for calculation of the peak normalized torsion-shear angle–volume change in early diastole ($-d\varphi'/dV'$). A, A schematic to depict the twist (T) and torsion shear-angle (φ). θ_{apex} and θ_{base} represent twist/untwist at apical and basal slices of the left ventricle (LV) at time (t), respectively. ρ_{apex} and ρ_{base} are the epicardial radii at apical and basal slices, respectively, and L is the distance between the apical and basal slices at end-diastole timeframe. (Schematic derived from Russel et al[20]). B and C, A representative example of short-axis of cine-CMR imaging without (B) and with (C) tagging grid. D and E, LV volume-time [V(t)] (D) and torsion shear-angle–time [φ(t)] (E) curves. In the graphs, time is measured from ECG R-wave. F, Torsion shear-angle change over time, normalized to its maximum [φ'(t)], and volume change over time, normalized to its maximum [V′(t)], are superimposed in 1 graph after time interpolation. The negative peak slope of the diastolic φ' vs V′ curve (ie, $-d\varphi'/dV'$) was calculated as the slope of a linear regression model fit to the first 4 points of the diastolic φ' vs V′ curve (red arrow).

Assessment of LV Chamber Stiffness

Based on measured LVEDP and LVEDV, a single-beat end-diastolic pressure-volume relationship was computed for each participant as previously described.[23-25] The chamber stiffness was defined as volume V at certain pressure P, computed as $V = e^{\frac{\log(\frac{P}{\alpha})}{\beta}}$, where α and β were functions of LVEDP and LVEDV.[23] The chamber stiffness constant β was calculated as recommended.[23,24] LVEDP/LVEDV ratio was also calculated and used as a surrogate estimate of LV chamber stiffness.[25]

Statistical Analysis

Data obtained during LV catheterization and CMR studies were analyzed offline in a blinded fashion. Normally distributed continuous variables were expressed as mean±SD and compared for those with and without LVDD using a 2-sided unpaired t test; otherwise variables were expressed as medians (interquartile range) and compared using a Mann-Whitney test (GraphPad Prism V.4.0.1, GraphPad, La Jolla, CA). Categorical variables were compared using a chi-squared test. Variables before and after NTG were compared using a paired t test. Linear regression analysis was performed to evaluate the correlations between CMR-derived LV torsion and invasive parameters. Receiver operating characteristic curve analysis was performed to identify the optimal thresholds of the $-d\varphi'/dV'$ for predicting abnormal τ-ME (>48 milliseconds), abnormal LVEDP (>12 mm Hg), and abnormal both τ-ME and LVEDP, (LVDD) using SPSS v. 23 (IBM, Armonk, NY). We obtained a 95% confidence interval (CI) for area under curve (AUC) of receiver operating characteristic and the *P*-value to test the null hypothesis that AUC=0.5 by nonparametric methods. The Youden index criterion was used to identify best cutoff value(s) from the receiver operating characteristic curve, and corresponding positive likelihood ratio and positive predictive values were calculated. A Bland-Altman plot was used to assess agreement between CMR-measured values at

baseline and after NTG treatment. A $P<0.05$ was considered statistically significant.

Results

Clinical Characteristics

Overall, study participants had NYHA functional class I and II symptoms: 89% of the total cohort had a history of chest pain; 64% had dyspnea. One-third had no significant CAD either on coronary angiogram or prior history of coronary revascularization. The prevalence of CAD did not differ between those with LVDD and without LVDD ("others"). One patient had atrial fibrillation with stable rhythm. There were no significant differences in the clinical characteristics of LVDD compared to others (Table 1).

LV Hemodynamic and Mechanical Characteristics

The mean LVEDP was 14.5±5.5 mm Hg, and τ-ME was 58±10 milliseconds (Table 2). Good correlation was noted between different τ methods and between τ and $T_{½}$

Table 1. Baseline Clinical Characteristics

	Overall	LVDD	Others
Number of patients, n	36	18	18
Age, y	61±7	62±5	60±8
Black/white, %	39/61	50/50	22/78
Male/female patients, %	86/14	78/22	94/6
Weight, kg	92±17	89±17	94±18
Body mass index, kg/m^2	29.6±5.0	29.9±5.4	29.4±4.7
Body surface area, m^2	2.1±0.2	2.0±0.2	2.1±0.2
Systolic blood pressure, mm Hg	131±17	129±18	132±16
Diastolic blood pressure, mm Hg	74±11	73±12	76±9
Hemoglobin, g/dL	13.6±1.7	13.2±1.2	14.0±2.0
Creatinine, mg/dL	0.95 (0.90-1.0)	0.95 (0.90-1.15)	0.95 (0.75-1.0)
NYHA class (I/II/III/IV), %	58/39/3/0	61/33/6/0	56/44/0/0
Fatigue/tiredness, %	69	72	67
Chest pain, %	89	94	89
Short of breath, %	64	61	67
Smoker, %	31	28	33
Hypertension, %	86	89	83
Diabetes mellitus, %	44	44	44
Dyslipidemia, %	86	78	94
COPD/lung disease, %	17	17	17
History of CHF, %	8	6	11
CAD, %	64	72	56
Major coronary occlusion (<30/30-70/>70), %	44/28/28	33/39/28	55/17/28
Medications, %			
AI/AT1RB/AA	56	44	67
Nitrates	31	22	39
α-Blockers	6	6	6
β-Blockers	64	67	61
Calcium channel blockers	19	17	22
Diuretics	42	33	50

Values are n or mean±SD or median (interquartile range). AA indicates aldosterone antagonist; AI, angiotensin-converting enzyme inhibitor; AT1RB, angiotensin II type-1 receptor blocker; CAD, coronary artery disease based on history and angiographic study; CHF, congestive heart failure; COPD, chronic obstructive pulmonary disease; LVDD, left ventricular diastolic dysfunction; NYHA, New York Heart Association.

Table 2. Hemodynamic and CMR Measurements

	Overall (N=36)	LVDD (N=18)	Others (N=18)
Hemodynamic measurements			
LV end-systolic pressure, mm Hg	127±18	129±16	125±20
LV minimum diastolic pressure, mm Hg	8.0±4.0	9.8±3.9	6.2±3.3†
LV end-diastolic pressure, mm Hg	14.5±5.5	17.4±3.4	11.5±5.7‡
LV end-diastolic wall stress, 1000 N/m^2	3.1±1.6	4.1±1.4	2.1±1.0‡
τ, monoexponential 0 asymptote, ms	58±10	64.1±6.8	51.7±8.3‡
τ, hybrid logistic, ms	38 (35-40)	39.1±2.1	33.5±8.6*
$T_{½}$, ms	44.3±6.8	48.3±3.4	40.3±7.0‡
LV end-diastolic pressure/volume ratio, mm Hg/mL	0.10 (0.07-0.13)	0.11 (0.10-0.15	0.08 (0.06-0.12)§
Chamber stiffness constant β	5.88 (5.78-6.01)	6.01 (5.94-6.13)	5.84 (5.72-5.88)‖
CMR measurements			
LV functionality			
LV ejection fraction, %	64±9	64±9	64±9
LV end-diastolic volume index, mL/m^2	66±15	73±13	59±13†
LV end-systolic volume index, mL/m^2	24±9	27±10	21±8
LV stroke volume index, mL/m^2	42±9	46±5	38±10†
LV mass index, g/m^2	53±11	51±12	55±1
LV mass/volume ratio, g/mL	0.85±0.27	0.72±0.18	0.98±0.30†
LV relative wall thickness	0.31±0.08	0.27±0.07	0.34±0.07*
Max left atrial volume index, mL/m^2	29±12	31±7	23 (17-31)§
LV strain			
Peak 2D circumferential shortening, %	11.3±2.9	12.3±2.6	10.2±2.9*
Early diastolic circumferential lengthening rate, %/s	96±39	105±38	86±38
LV torsion			
Peak twist rate, °/s	59±16	59±16	58±17
Time to peak twist rate, ms	140±35	139±28	142±42
Peak untwist rate, °/s	54±15	58±10	51±18
Time to peak untwist rate, ms	399±77	383±59	416±91
Peak twist per length rate, °/cm·s	14.7±3.8	15.4±3.7	14.0±3.8
Peak untwist per length rate, °/cm·s	13.7±3.7	15.2±2.7	12.2±4.0
$-d\varphi'/dV'$	5.6±3.7	7.6±4.2	3.6±1.6†

Values are mean±SD or median (interquartile range). CMR indicates cardiovascular magnetic resonance imaging; $-d\varphi'/dV'$, peak normalized torsion-shear angle–volume change in early diastole; LV, left ventricular; LVDD, LV diastolic dysfunction; Max, maximum; ms, milliseconds; $T_{½}$, half-time of LV relaxation; τ, time constant of LV relaxation; 2D, 2-dimensional.
*P<0.05, †P<0.01, ‡P<0.001 vs LVDD by unpaired t test.
§P<0.05, ‖P<0.001 vs LVDD by Mann-Whitney test.

(Figure S1). Twenty-nine (81%) had τ-ME >48 milliseconds, and 22 (61%) had LVEDP >12 mm Hg. No significant linear relationship between LVEDP and τ-ME was found (r=0.22, P=0.20). Eighteen (50%) had LVDD defined by elevated LVEDP and τ-ME (Figure 3). Three (8%) had normal LVEDP and τ, and 15 (42%) had either elevated LVEDP or prolonged τ-ME. On secondary analysis, no significant difference in coronary stenosis or CAD was found in LVDD compared to the other group (Figure S2). LV end-diastolic stress was increased in LVDD compared with others (Table 2). Single-beat chamber stiffness constant β and LVEDP/LVEDV ratio were significantly higher in LVDD compared with others (Table 2).

CMR LV Quantification

On CMR, mean LVEF was 64±9% (Table 2). The LV mass and volume index were within normal limits. LVDD had

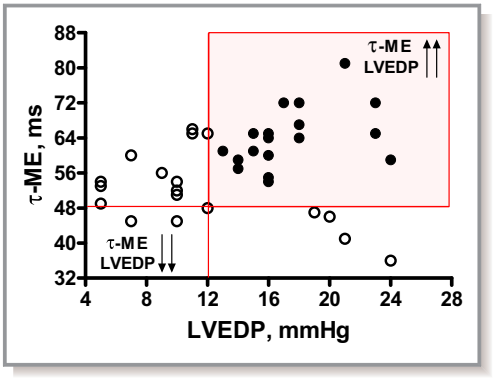

Figure 3. Scatterplot of left ventricular end-diastolic pressure (LVEDP) and time constant of LV relaxation (monoexponential model with 0 asymptote, τ-ME). Red lines separate participants with normal vs elevated LVEDP (≤12 and >12 mm Hg) and participants with normal vs prolonged τ-ME (≤48 ms and >48 ms). Red square depicts LVDD participants.

larger LV volumes and lower LV relative wall thickness and LV mass/volume ratio. Mean left atrial volume index was higher in those with LVDD compared with others (Table 2). The LV systolic circumferential shortening was higher in LVDD, but early diastolic strain rate was similar in both groups (Table 2). The peak systolic twist rate and the peak untwist rate were not significantly different in LVDD (Table 2). When spatially normalized, the difference in the peak untwist per length rates between groups reached a significant level (P=0.014, Table 2). The peak twist rates and the peak untwist rates were correlated (r=0.42, P=0.011 and, for spatially normalized values, r=0.37, P=0.029, n=36). The peak untwist rate significantly correlated to LVEDV (r=0.44, P=0.008), and the peak untwist per length rate significantly correlated to mass/volume ratio (r=−0.44, P=0.007).

Diagnostic Value of $-d\varphi'/dV'$ to Predict Abnormal LVEDP, τ-ME, and LVDD

The mean $-d\varphi'/dV'$ was 5.6±3.7, and $-d\varphi'/dV'$ was significantly higher in LVDD compared with others (P=0.001, Table 2). No significant correlation between $-d\varphi'/dV'$ and LV structural characteristics, including LV volume, mass, or LV mass/volume ratio, was found (not shown).

There was a significant correlation of $-d\varphi'/dV'$ with τ-ME (r=0.37, P<0.05, Figure 4A) and with LVEDP (r=0.36, P<0.05, Figure 4B). On secondary analysis, $-d\varphi'/dV'$ was similar for participants with or without CAD (Figure S3). Participants with τ-ME >48 milliseconds had significantly higher $-d\varphi'/dV'$ values than participants with τ-ME ≤48 milliseconds (6.1±0.7 versus 3.5±0.6, P<0.05). Similarly, those with LVEDP >12 mm Hg had higher values of $-d\varphi'/dV'$ than participants with LVEDP ≤12 mm Hg (6.7±0.9 versus 3.8±0.4, P<0.05). Receiver operating characteristic analysis indicated that $-d\varphi'/dV'$ had AUC of 0.72 (95% CI=0.55-0.89, P=0.028) to identify LVEDP >12 mm Hg (Figure 4C and 4D). At $-d\varphi'/dV'$ cutoff ≥5.5, sensitivity was 64%, and specificity was 93%, whereas $-d\varphi'/dV'$ ≥6.2 had sensitivity 59% and specificity 100% (Figure 4E). $-d\varphi'/dV'$ had AUC of 0.72 (95% CI=0.54-0.89, P=0.075) for identifying Tau >48 milliseconds, with 52% sensitivity and 100% specificity at $-d\varphi'/dV'$ cutoff ≥5.5 (Figure 4E). Furthermore, AUC for $-d\varphi'/dV'$ to identify LVDD was 0.83 (95% CI=0.67-0.98, P=0.001, Figure 4E). At $-d\varphi'/dV'$ cutoff ≥5.5, the sensitivity and specificity of $-d\varphi'/dV'$ to identify LVDD were 78% and 94%, respectively, with a positive likelihood ratio of 13.9 and a positive predictive value of 93% (Figure 4E). For $-d\varphi'/dV'$ ≥6.2, sensitivity was 72%, and specificity was 100%.

AUC for $-d\varphi'/dV'$ to identify LVDD cohort defined on alternative LVEDP threshold (τ-ME >48 milliseconds and LVEDP >16 mm Hg) is also high (Figure S4). $-d\varphi'/dV'$ values for participants without LVDD (τ-ME ≤48 milliseconds and/or LVEDP ≤12 mm Hg), for those with LVDD but LVEDP ≤16 mm Hg (τ-ME >48 milliseconds and LVEDP of 13-16 mm Hg), and for those with LVDD but LVEDP >16 mm Hg (τ-ME >48 milliseconds and LVEDP >16 mm Hg) increased in stepwise fashion (3.6±1.6, n=18 versus 6.2±3.1, n=10 versus 9.3±4.9, n=8, P<0.001 by one-way ANOVA with P<0.001 for linear trend posttest).

We found that for participants with elevated LVEDP (>12 mm Hg), $-d\varphi'/dV'$ was higher in participants with prolonged τ-ME (>48 milliseconds) (Figure S5). Among participants with prolonged τ-ME, those who also had elevated LVEDP were associated with significantly higher $-d\varphi'/dV'$ and even more prolonged τ-ME. The same was true when subjects were grouped based on alternative LVEDP threshold (≤ or >16 mm Hg) (Figure S5). These results suggest that the rise of $-d\varphi'/dV'$ reflects a highly impaired early diastolic relaxation (as measured by greatly prolonged τ-ME), which is accompanied with impaired LV passive compliance (as measured by elevated LVEDP).

Hemodynamic and $-d\varphi'/dV'$ Measurements Following NTG Administration

Sublingual NTG treatment had no significant hemodynamic effect in the treated cohort (Table 3). There was no difference in $-d\varphi'/dV'$ values before and after NTG treatment. Values of $-d\varphi'/dV'$ before and after NTG correlated well (r=0.77, P<0.001) and were consistent on Bland-Altman plots (Figure 5). Post-NTG, $-d\varphi'/dV'$ remained significantly higher in LVDD (Table 4).

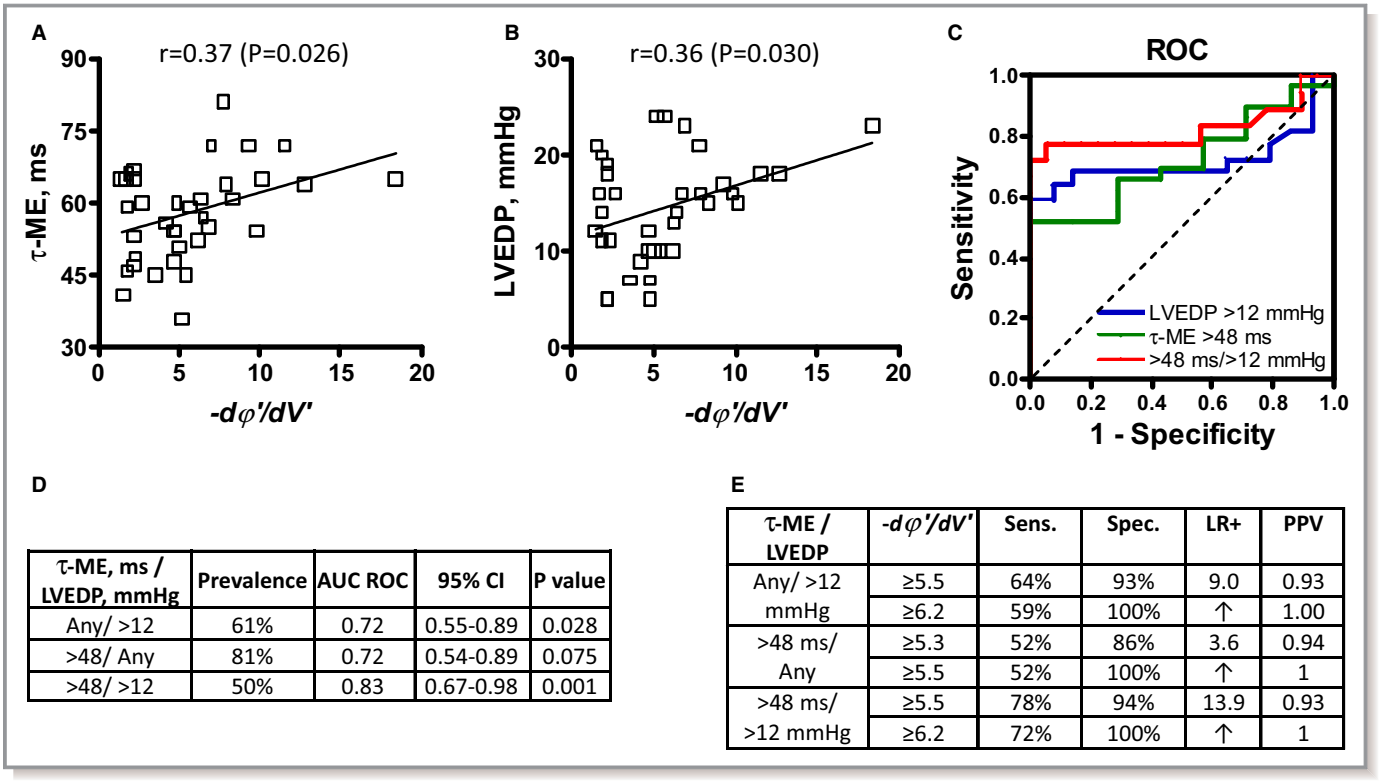

D

τ-ME, ms / LVEDP, mmHg	Prevalence	AUC ROC	95% CI	P value
Any/ >12	61%	0.72	0.55-0.89	0.028
>48/ Any	81%	0.72	0.54-0.89	0.075
>48/ >12	50%	0.83	0.67-0.98	0.001

E

τ-ME / LVEDP	-dφ′/dV′	Sens.	Spec.	LR+	PPV
Any/ >12 mmHg	≥5.5	64%	93%	9.0	0.93
	≥6.2	59%	100%	↑	1.00
>48 ms/ Any	≥5.3	52%	86%	3.6	0.94
	≥5.5	52%	100%	↑	1
>48 ms/ >12 mmHg	≥5.5	78%	94%	13.9	0.93
	≥6.2	72%	100%	↑	1

Figure 4. Diagnostic accuracy of −dφ′/dV′ to identify left ventricular (LV) diastolic dysfunction (LVDD). A and B, Linear regression between −dφ′/dV′ and LV end-diastolic pressure (LVEDP) and time constant of LV relaxation (monoexponential model with 0 asymptote, τ-ME), respectively. C, Receiver operating characteristic (ROC) curves for −dφ′/dV′ to identify elevated LVEDP (>12 mm Hg), prolonged τ-ME (>48 ms), and LVDD. Corresponding condition prevalence and area under the curve (AUC) estimates with 95% confidence interval (CI) and *P*-value vs AUC of 0.5 are shown in D, and sensitivity, specificity, positive likelihood ratio (LR+), and positive predictive value (PPV) for optimal −dφ′/dV′ cutoffs are shown in E. ↑ indicates indefinitely high; ms, milliseconds.

Alternative Methods for Calculating −dφ′/dV′

Interval and regression harmonic phase–based calculation of −dφ′/dV′ values were almost identical (5.73±4.12 and 5.59±3.74, n=36, respectively) and linearly correlated (r=0.99, P<0.001). Values of −dφ′/dV′ calculated using FAST and harmonic phase methods were similar (5.0±3.5 versus 5.6±3.7, n=36, P=0.47). They are well correlated (r=0.77, P<0.001) and closely matched according to the Bland-Altman plot (Figure S6). FAST method calculated −dφ′/dV′ identified LVDD with AUC of 0.79 (95% CI=0.64-0.95, P=0.003, Figure S6).

Discussion

In the current study we demonstrated that the rate of change of LV torsion shear angle (φ′) normalized to the corresponding rate of change in LV volume (V′) during early diastole (−dφ′/dV′) correlates with LVEDP and LV diastolic relaxation rate and identifies invasively confirmed LVDD.

τ, a parameter for measuring isovolumic LV relaxation rate, characterizes early diastolic abnormality while LVEDP quantifies the overall effect of LV filling on the left ventricle. In combination, these parameters are an indication of myofilament crossbridge uncoupling and LV chamber properties. Therefore, impaired LV relaxation (ie, prolonged τ) along with elevated LVEDP accurately characterizes LVDD on invasive measurements.[2] This is consistent with increased end-diastolic wall stress and increased LV chamber stiffness in the LVDD group. We find that CMR-derived peak early diastolic −dφ′/dV′ is increased in LVDD. Increased −dφ′/dV′ indicates impaired LV filling for similar LV untwist in LVDD. It has been previously demonstrated that untwist correlates with the gradient across the mitral valve and influences early LV filling and diastolic function.[26,27] Our results are consistent with our previous article in which we hypothesized that increased peak early diastolic −dφ′/dV′ in suspected diastolic dysfunction suggests impaired ventricular relaxation.[10] Because −dφ′/dV′ is normalized based on peak systolic torsion-shear strain, it accounts for subtle differences in systolic function that may be present in LVDD despite preserved LVEF. Furthermore, −dφ′/dV′ is a global parameter in that it evaluates the whole left ventricle and therefore possibly can be applied regardless of LV remodeling. No

Table 3. Hemodynamic Variables and CMR-Derived $-d\varphi'/dV'$ at Baseline and After Nitroglycerin

Variables	Baseline (N=32)	Nitroglycerin (N=32)	Difference (N=32)	*P* Value
LV end-systolic pressure, mm Hg	128±17.7	126±18.2	−1.2±9.1	0.47
LV end-diastolic pressure, mm Hg	14.4±5.4	13.9±5.6	−0.5±3.7	0.43
LV minimum diastolic pressure, mm Hg	7.8±3.7	7.2±4.4	−0.6±2.8	0.28
τ-ME, ms	57.4±9.5	56.3±11.3	−1.1±6.1	0.36
$-d\varphi'/dV'$	5.8±3.8	5.9±3.7	0.04±2.52	0.92

Values are mean±SD. Variables at baseline and after nitroglycerin were compared using 2-tailed paired t test. CMR indicates cardiovascular magnetic resonance imaging; $-d\varphi'/dV'$, peak normalized torsion-shear angle–volume changes in early diastole; LV, left ventricular; ms, milliseconds; τ-ME, time constant of LV relaxation (monoexponential model with 0 asymptote).

significant relationship between $-d\varphi'/dV'$ and LV structural characteristics was found in our study. This is also made evident by higher $-d\varphi'/dV'$ in our invasively proven LVDD group, which demonstrated increased end-diastolic LV wall stress and chamber stiffness but no concentric remodeling. However, further research is required to evaluate additional mechanisms that may be contributing to the observed differences.

Previous investigators have suggested reduced LV untwist in isovolumic phase as a useful parameter to quantify impaired LV relaxation.[27-31] Here, due to lower temporal resolution of tagged CMR, peak untwist rate during isovolumic relaxation period cannot be measured. Rather, the untwist rate and peak untwist per length rate in our study relate to overall LV untwist in the early diastolic phase that includes LV filling following mitral valve opening. We found that peak untwist rate is not significantly different; however, the spatially normalized peak untwist rate is increased in the LVDD group. Normalized peak untwist rate correlates with peak systolic twist and LV mass/volume ratio. This suggests that, in addition to relaxation and restoration forces, other factors including LV volume, pressure, and mass may be contributing to the LV untwist.[28,30,31] Other investigators have also demonstrated a relationship of untwist to LV mass and remodeling similar to our work.[28,30] Moreover, in a canine study, the investigators have found that the peak untwist rate was increased with an increase in τ and LV pressure at the mitral valve opening in cases of volume overloading alone.[31] In a human study, investigators have demonstrated increased isovolumic untwist rate after increased preload.[32] In our study we also find larger LV volumes along with elevated τ and LV minimum diastolic pressure in LVDD, suggesting that LV preload may be playing a role in increased untwist rate. On the other hand, no relationship between $-d\varphi'/dV'$ and LV volumetric or structural characteristics was found. LV volumes in the present study cohort were in the normal range,[33] and LV volumes seemed not to play any role in the $-d\varphi'/dV'$ increase in our previous study.[10] Additional studies incorporating pressure and volume overload condition on $-d\varphi'/dV'$ can further elucidate this mechanism.

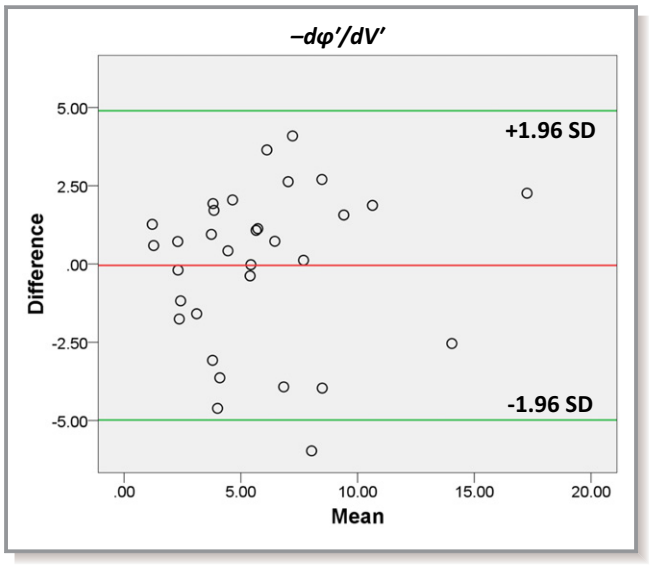

Figure 5. Bland-Altman plot for assessment of corresponding values of $-d\varphi'/dV'$ at baseline and after nitroglycerin intake (n=32).

Our participant cohort represents a particularly challenging patient population who frequently present with heart failure risk factors and limited signs and symptoms suggesting LVDD. Echocardiography remains the first-line diagnostic test to evaluate such patients.[3,34] However, the American Society of Echocardiography recommended evaluating algorithms[3,34] require prospective validation in multicenter studies.[35] Recently, good agreement between LV strain-volume analysis by tagged CMR and echocardiography speckle tracking was demonstrated.[36] Our proposed method may therefore be extended to echocardiography after prospective validation in evaluation of LVDD.

There are limitations that should be taken into account for interpretation of the results of this work. Our study population were comprised of clinically stable participants who were referred to cardiac catheterization due to chest pain and/or dyspnea (NYHA class I-II) to exclude CAD; therefore, we acknowledge the potential presence of referral bias in the study. We believe that our cohort consists of patients frequently seen in ambulatory clinics, where a definitive diagnosis is frequently not made. We did not have a completely normal cohort or a cohort with an established heart failure with preserved ejection fraction diagnosis. The present work therefore needs to be extended to include these

Table 4. Comparison of Hemodynamic Variables and CMR-Derived $-d\varphi'/dV'$ in 2 Groups (LVDD vs Others) at Baseline and After Nitroglycerin

	Baseline		Nitroglycerin	
Variables	LVDD (N=16)	Others (N=16)	LVDD (N=16)	Others (N=16)
LV end-systolic pressure, mm Hg	129±16	126±20	128±17	125±20
LV end-diastolic pressure, mm Hg	17.0±3.2	11.9±6.0†	16.2±4.9	11.6±5.4*
LV minimum diastolic pressure, mm Hg	9.2±3.8	6.4±3.2*	8.5±4.3	5.6±4.0*
τ-ME, ms	63.4±7.0	51.4±7.9†	62.6±7.6	50.1±11.2†
$-d\varphi'/dV'$	8.0±4.3	3.7±1.6†	7.3±4.0	4.5±2.7*

Values are mean±SD. CMR indicates cardiovascular magnetic resonance imaging; $-d\varphi'/dV'$, peak normalized torsion-shear angle–volume changes in early diastole; LV, left ventricular; LVDD, LV diastolic dysfunction; ms, milliseconds; τ-ME, time constant of LV relaxation (monoexponential model with 0 asymptote).
*P<0.05, †P<0.01 vs corresponding LVDD group by 2-tailed unpaired t test. There were no statistically significant differences for LVDD or Others at baseline and after nitroglycerin intake (paired t test was used for comparison).

cohorts to evaluate our proposed approach. We did not perform simultaneous CMR with invasive procedure as logistically it was not possible in our present setup. Our approach for LVDD definition relied on 2 LV hemodynamic parameters (LVEDP and τ), which are potentially vulnerable to hemodynamic fluctuations. However, we also performed the same CMR measurements after sublingual NTG administration and found that $-d\varphi'/dV'$ measurements remained consistent, suggesting that our measurements are robust and not adversely affected by loading conditions. Further, we quantified LV mechanical stiffness, which was consistently abnormal in LVDD. We have previously demonstrated no significant inter- and intraobserver variability in the contour propagation algorithm used in the present study.[14] We analyzed our data in a blinded fashion. We also found consistent results using different analytical methods for CMR quantification. Our study results also remained consistent regardless of the presence/absence of CAD based on angiographic assessment of the severity of coronary stenosis. The study was conducted under resting conditions, and thus, no significant resting myocardium ischemia was expected. The present work is a single-center study with a limited but well-defined cohort. The results need to be validated in a larger prospective study. Because the present work has been exploratory with a single outcome of our primary interest ($-d\varphi'/dV'$), we have not adjusted *P*-values for multiple comparisons. This is the best approach in order to promote hypothesis generation for future studies.

Conclusion

In conclusion, we demonstrate a novel method using tagged CMR that identifies elevated LV filling pressure and abnormal LV relaxation in preserved LVEF and therefore can be useful to evaluate LVDD. This requires a larger clinical study for confirmation of our findings.

Acknowledgments

We want to acknowledge the faculty members of the section of interventional cardiology who helped with acquisition of invasive parameters.

Sources of Funding

The study was supported by a National Institutes of Health National Heart, Lung and Blood Institute R01-HL104018 grant. The funding organizations did not have any role in the design or conduct of the study; collection, management, analysis, or interpretation of the data; or preparation, review, or approval of the manuscript; or with the decision to submit the manuscript for publication.

Disclosures

None.

References

1. Kane GC, Karon BL, Mahoney DW, Redfield MM, Roger VL, Burnett JC Jr, Jacobsen SJ, Rodeheffer RJ. Progression of left ventricular diastolic dysfunction and risk of heart failure. *JAMA*. 2011;306:856–863.
2. Paulus WJ, Tschope C, Sanderson JE, Rusconi C, Flachskampf FA, Rademakers FE, Marino P, Smiseth OA, De Keulenaer G, Leite-Moreira AF, Borbely A, Edes I, Handoko ML, Heymans S, Pezzali N, Pieske B, Dickstein K, Fraser AG, Brutsaert DL. How to diagnose diastolic heart failure: a consensus statement on the diagnosis of heart failure with normal left ventricular ejection fraction by the Heart Failure and Echocardiography Associations of the European Society of Cardiology. *Eur Heart J*. 2007;28:2539–2550.
3. Nagueh SF, Smiseth OA, Appleton CP, Byrd BF III, Dokainish H, Edvardsen T, Flachskampf FA, Gillebert TC, Klein AL, Lancellotti P, Marino P, Oh JK, Popescu BA, Waggoner AD. Recommendations for the evaluation of left ventricular diastolic function by echocardiography: an update from the American Society of Echocardiography and the European Association of Cardiovascular Imaging. *J Am Soc Echocardiogr*. 2016;29:277–314.
4. Santos M, Rivero J, McCullough SD, West E, Opotowsky AR, Waxman AB, Systrom DM, Shah AM. E/e′ ratio in patients with unexplained dyspnea: lack of accuracy in estimating left ventricular filling pressure. *Circ Heart Fail*. 2015;8:749–756.
5. Sharifov OF, Schiros CG, Aban I, Denney TS, Gupta H. Diagnostic accuracy of tissue Doppler index E/e′ for evaluating left ventricular filling pressure and

diastolic dysfunction/heart failure with preserved ejection fraction: a systematic review and meta-analysis. *J Am Heart Assoc*. 2016;5:e002530. DOI: 10.1161/JAHA.115.002530.

6. Omar AM, Vallabhajosyula S, Sengupta PP. Left ventricular twist and torsion: research observations and clinical applications. *Circ Cardiovasc Imaging*. 2015;8:e003029.
7. Ahmed MI, Desai RV, Gaddam KK, Venkatesh BA, Agarwal S, Inusah S, Lloyd SG, Denney TS Jr, Calhoun D, Dell'italia LJ, Gupta H. Relation of torsion and myocardial strains to LV ejection fraction in hypertension. *JACC Cardiovasc Imaging*. 2012;5:273–281.
8. Sengupta PP, Tajik AJ, Chandrasekaran K, Khandheria BK. Twist mechanics of the left ventricle: principles and application. *JACC Cardiovasc Imaging*. 2008;1:366–376.
9. Young AA, Cowan BR. Evaluation of left ventricular torsion by cardiovascular magnetic resonance. *J Cardiovasc Magn Reson*. 2012;14:49.
10. Schiros CG, Desai RV, Venkatesh BA, Gaddam KK, Agarwal S, Lloyd SG, Calhoun DA, Denney TS Jr, Dell'italia LJ, Gupta H. Left ventricular torsion shear angle volume analysis in patients with hypertension: a global approach for LV diastolic function. *J Cardiovasc Magn Reson*. 2014;16:70.
11. Weiss JL, Frederiksen JW, Weisfeldt ML. Hemodynamic determinants of the time-course of fall in canine left ventricular pressure. *J Clin Invest*. 1976;58:751–760.
12. Senzaki H, Fetics B, Chen CH, Kass DA. Comparison of ventricular pressure relaxation assessments in human heart failure: quantitative influence on load and drug sensitivity analysis. *J Am Coll Cardiol*. 1999;34:1529–1536.
13. Castillo E, Osman NF, Rosen BD, El-Shehaby I, Pan L, Jerosch-Herold M, Lai S, Bluemke DA, Lima JA. Quantitative assessment of regional myocardial function with MR-tagging in a multi-center study: interobserver and intraobserver agreement of fast strain analysis with harmonic phase (HARP) MRI. *J Cardiovasc Magn Reson*. 2005;7:783–791.
14. Feng W, Nagaraj H, Gupta H, Lloyd SG, Aban I, Perry GJ, Calhoun DA, Dell'Italia LJ, Denney TS Jr. A dual propagation contours technique for semi-automated assessment of systolic and diastolic cardiac function by CMR. *J Cardiovasc Magn Reson*. 2009;11:30.
15. Schiros CG, Dell'Italia LJ, Gladden JD, Clark D III, Aban I, Gupta H, Lloyd SG, McGiffin DC, Perry G, Denney TS Jr, Ahmed MI. Magnetic resonance imaging with 3-dimensional analysis of left ventricular remodeling in isolated mitral regurgitation: implications beyond dimensions. *Circulation*. 2012;125:2334–2342.
16. Schiros CG, Ahmed MI, McGiffin DC, Zhang X, Lloyd SG, Aban I, Denney TS Jr, Dell'Italia LJ, Gupta H. Mitral annular kinetics, left atrial, and left ventricular diastolic function post mitral valve repair in degenerative mitral regurgitation. *Front Cardiovasc Med*. 2015;2:31.
17. Osman NF, Kerwin WS, McVeigh ER, Prince JL. Cardiac motion tracking using CINE harmonic phase (HARP) magnetic resonance imaging. *Magn Reson Med*. 1999;42:1048–1060.
18. Khalifa A, Youssef AB, Osman N. Improved harmonic phase (HARP) method for motion tracking a tagged cardiac MR images. *Conf Proc IEEE Eng Med Biol Soc*. 2005;4:4298–4301.
19. Thompson RB, Paterson I, Chow K, Cheng-Baron J, Scott JM, Esch BT, Ennis DB, Haykowsky MJ. Characterization of the relationship between systolic shear strain and early diastolic shear strain rates: insights into torsional recoil. *Am J Physiol Heart Circ Physiol*. 2010;299:H898–H907.
20. Russel IK, Tecelao SR, Kuijer JP, Heethaar RM, Marcus JT. Comparison of 2D and 3D calculation of left ventricular torsion as circumferential-longitudinal shear angle using cardiovascular magnetic resonance tagging. *J Cardiovasc Magn Reson*. 2009;11:8.
21. Reyhan M, Natsuaki Y, Ennis DB. Fourier analysis of stimulated echoes (FAST) for the quantitative analysis of left ventricular twist. *J Magn Reson Imaging*. 2012;35:587–593.
22. Kern MJ, Sorajja P, Lin M, eds. *The Cardiac Catheterization Handbook*. Philadelphia, PA: Elsevier; 2016:e12. Appendix D-6.
23. Klotz S, Dickstein ML, Burkhoff D. A computational method of prediction of the end-diastolic pressure-volume relationship by single beat. *Nat Protoc*. 2007;2:2152–2158.
24. Ten Brinke EA, Burkhoff D, Klautz RJ, Tschope C, Schalij MJ, Bax JJ, van der Wall EE, Dion RA, Steendijk P. Single-beat estimation of the left ventricular end-diastolic pressure-volume relationship in patients with heart failure. *Heart*. 2010;96:213–219.
25. Kasner M, Sinning D, Burkhoff D, Tschope C. Diastolic pressure-volume quotient (DPVQ) as a novel echocardiographic index for estimation of LV stiffness in HFpEF. *Clin Res Cardiol*. 2015;104:955–963.
26. Yellin E, Nikolic S. Diastolic function and the dynamics of left ventricular filling. In: Gaasch W, LeWinter M, eds. *Left Ventricular Diastolic Dysfunction and Heart Failure*. Malvern, PA: Lea&Febiger; 1994:69–102.
27. Notomi Y, Popovic ZB, Yamada H, Wallick DW, Martin MG, Oryszak SJ, Shiota T, Greenberg NL, Thomas JD. Ventricular untwisting: a temporal link between left ventricular relaxation and suction. *Am J Physiol Heart Circ Physiol*. 2008;294:H505–H513.
28. Takeuchi M, Borden WB, Nakai H, Nishikage T, Kokumai M, Nagakura T, Otani S, Lang RM. Reduced and delayed untwisting of the left ventricle in patients with hypertension and left ventricular hypertrophy: a study using two-dimensional speckle tracking imaging. *Eur Heart J*. 2007;28:2756–2762.
29. Dong SJ, Hees PS, Siu CO, Weiss JL, Shapiro EP. MRI assessment of LV relaxation by untwisting rate: a new isovolumic phase measure of tau. *Am J Physiol Heart Circ Physiol*. 2001;281:H2002–H2009.
30. Burns AT, La Gerche A, Prior DL, Macisaac AI. Left ventricular untwisting is an important determinant of early diastolic function. *JACC Cardiovasc Imaging*. 2009;2:709–716.
31. Opdahl A, Remme EW, Helle-Valle T, Edvardsen T, Smiseth OA. Myocardial relaxation, restoring forces, and early-diastolic load are independent determinants of left ventricular untwisting rate. *Circulation*. 2012;126:1441–1451.
32. Weiner RB, Weyman AE, Khan AM, Reingold JS, Chen-Tournoux AA, Scherrer-Crosbie M, Picard MH, Wang TJ, Baggish AL. Preload dependency of left ventricular torsion: the impact of normal saline infusion. *Circ Cardiovasc Imaging*. 2010;3:672–678.
33. Kawel-Boehm N, Maceira A, Valsangiacomo-Buechel ER, Vogel-Claussen J, Turkbey EB, Williams R, Plein S, Tee M, Eng J, Bluemke DA. Normal values for cardiovascular magnetic resonance in adults and children. *J Cardiovasc Magn Reson*. 2015;17:29.
34. Nagueh SF, Appleton CP, Gillebert TC, Marino PN, Oh JK, Smiseth OA, Waggoner AD, Flachskampf FA, Pellikka PA, Evangelista A. Recommendations for the evaluation of left ventricular diastolic function by echocardiography. *J Am Soc Echocardiogr*. 2009;22:107–133.
35. Galderisi M, Lancellotti P, Donal E, Cardim N, Edvardsen T, Habib G, Magne J, Maurer G, Popescu BA. European multicentre validation study of the accuracy of E/e' ratio in estimating invasive left ventricular filling pressure: EURO-FILLING study. *Eur Heart J Cardiovasc Imaging*. 2014;15:810–816.
36. Lilli A, Tessa C, Diciotti S, Croisille P, Clarysse P, Del Meglio J, Salvatori L, Vignali C, Casolo G. Simultaneous strain-volume analysis by three-dimensional echocardiography: validation in normal subjects with tagging cardiac magnetic resonance. *J Cardiovasc Med (Hagerstown)*. 2017;18:223–229.

SUPPLEMENTAL MATERIAL

Figure S1. Relationship between different assessments of LV relaxation rate

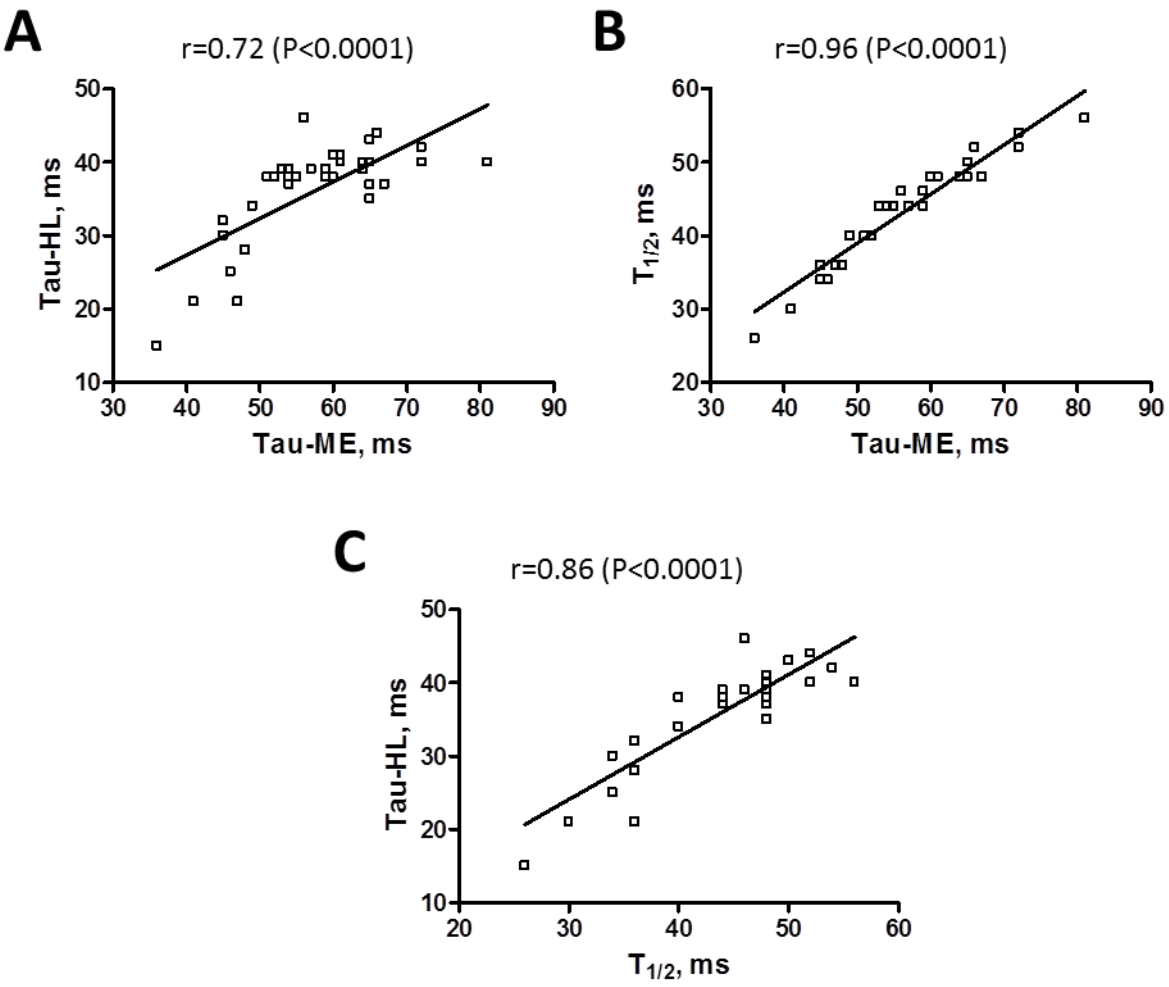

Good linear correlation was noted between mono-exponential (ME) and hybrid logistic (HL) methods to calculate time constant of LV relaxation, Tau, (**A**) and also between Tau-ME and $T_{1/2}$ (**B**), and between Tau-HL and $T_{1/2}$ (**C**).

Figure S2. Relation of hemodynamic parameters to CAD

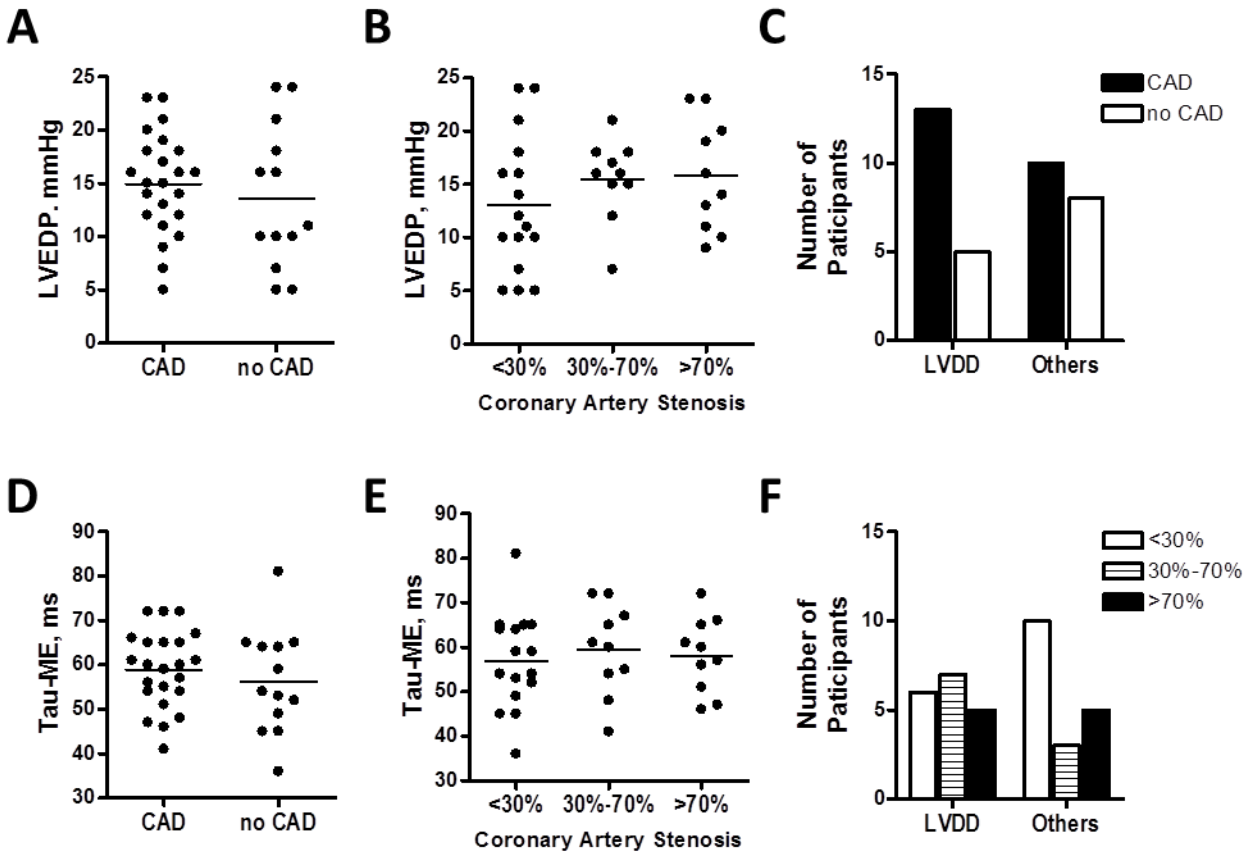

LVEDP (**A, B**) and Tau-ME (**D,E**) distribution based on presence or absence of CAD and severity of coronary artery stenosis is depicted. Severity of coronary artery stenosis was based on the observed stenosis in right, left main, left anterior descending and/or left circumflex coronary arteries during coronary angiogram. There was no relation of hemodynamic parameters to the presence/absence of CAD or the severity of coronary stenosis. Overall, presence of CAD (**C**) and severity of coronary artery stenosis (**F**) was similar in LVDD compared to others.

Figure S3. Relation of -*dφ'*/d*V'* to CAD

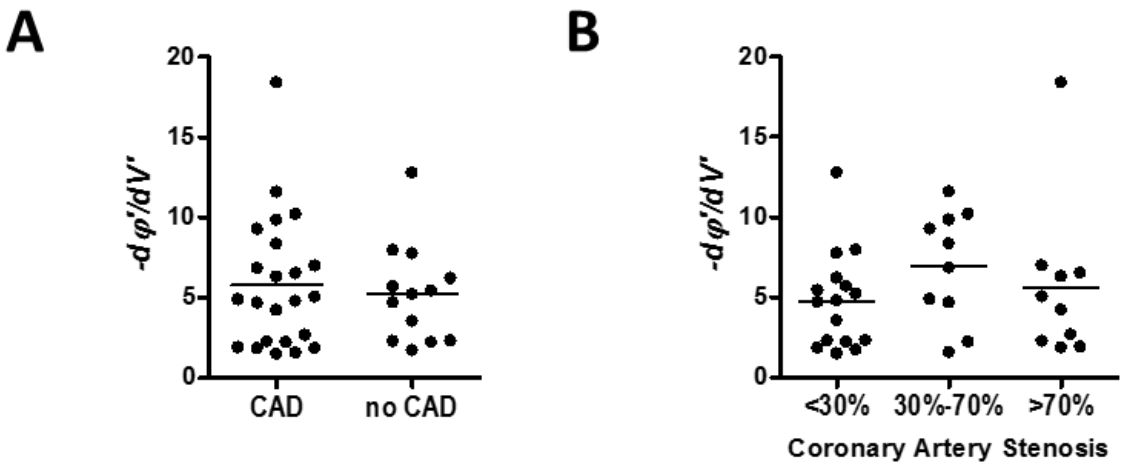

Distribution of CMR-derived *-dφ'/dV'* (**A,B**) is depicted based on presence or absence of CAD and severity of coronary artery stenosis. Severity of coronary artery stenosis was based on the observed stenosis in right, left main, left anterior descending and/or left circumflex coronary arteries during coronary angiogram. There was no relation of CMR *-dφ'/dV'* to the presence/absence of CAD or the severity of coronary stenosis.

Figure S4. ROC analysis for *-dφ'/dV'* to identify LVDD for LVEDP >16 mmHg

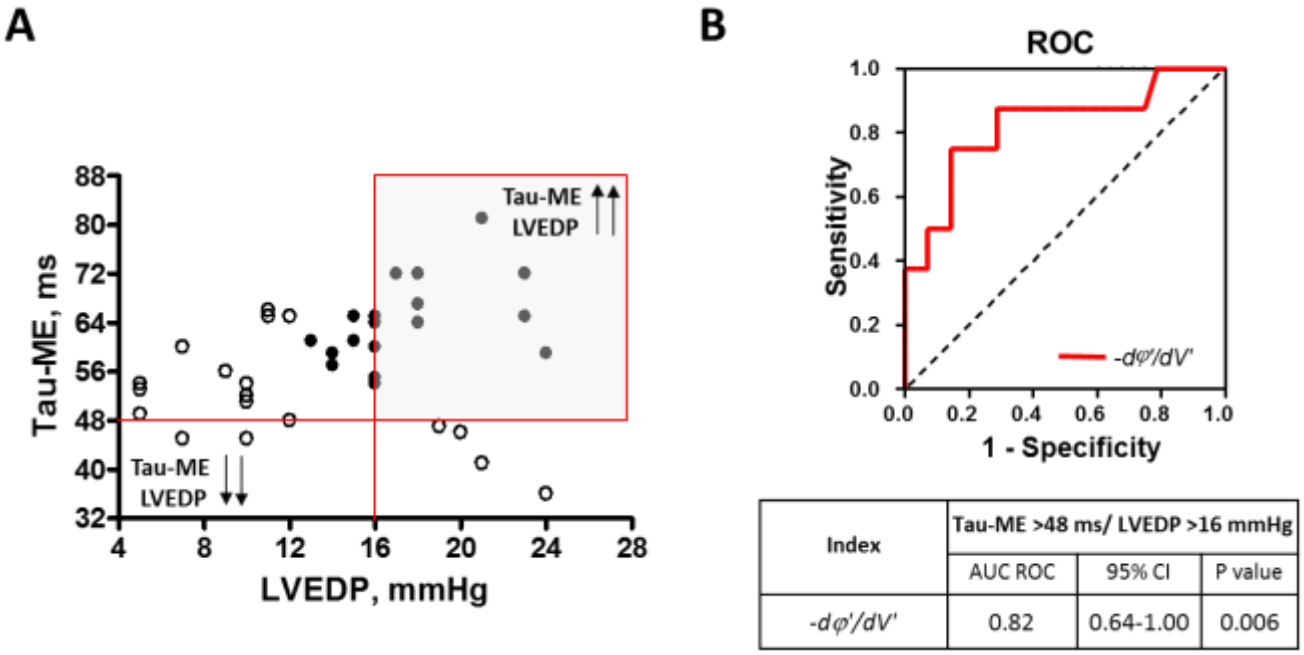

Index	Tau-ME >48 ms/ LVEDP >16 mmHg		
	AUC ROC	95% CI	P value
-dφ'/dV'	0.82	0.64-1.00	0.006

A: Scatterplot of LVEDP and Tau-ME. Red lines separates participants with elevated vs. normal LVEDP at alternative threshold (≤16 mmHg and >16 mmHg) and participants with prolonged vs. normal Tau-ME (≤48 ms and >48 ms). Red square depicts definite LVDD participants (n=8) with concurrently abnormal LVEDP and Tau-ME. **B**: ROC analysis (AUC estimates with 95%CI and P-value vs. AUC of 0.5) for *-dφ'/dV'* to identify LVDD defined by alternative LVEDP threshold (>16 mmHg) and Tau-ME >48 ms.

We find consistent results for identifying alternative LVDD using --*dφ'/dV'*. At *-dφ'/dV'* cutoff ≥5.5, the sensitivity and specificity of *-dφ'/dV'* to identify LVDD was 88% and 71%. At *-dφ'/dV'* ≥6.2, sensitivity was 75% and specificity was 75%. At *-dφ'/dV'* ≥6.9, sensitivity was 75% and specificity was 86%, and at *-dφ'/dV'* ≥10.9, sensitivity was 38% and specificity was 100%

Figure S5. Distribution of *-dφ'/dV'*, LVEDP and Tau-ME in subgroups

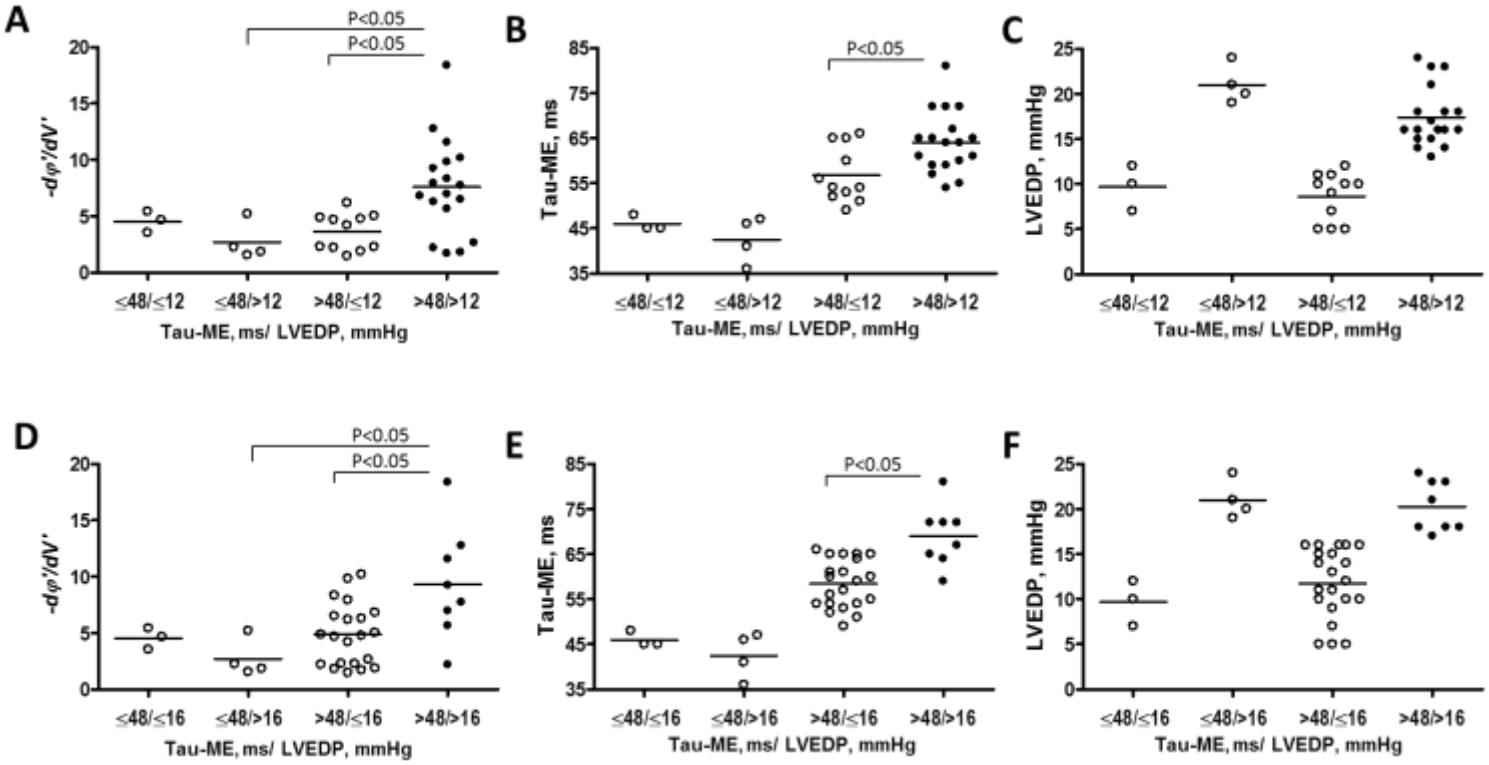

-dφ'/dV', Tau-ME and LVEDP values are depicted for specific Tau-ME/LVEDP groups. **A,B,C**: Subjects were grouped based on Tau-ME (≤ or > 48 md) and LVEDP (≤ or > 12 mmHg). LVDD (Tau-ME>48 ms and LVEDP>12 mmHg, solid dots), was compared to 'others' (Tau-ME ≤48 ms and/or LVEDP ≤12 mmHg, open dots). **D,E,F**: Subjects were grouped based on Tau-ME (≤ or > 48 md) and LVEDP (≤ or > 16 mmHg).

For participants with elevated LVEDP, *-dφ'/dV'* was higher in participants with prolonged Tau-ME (shown in A, ≤48/> 12 vs. >48/>12, P<0.05). Amongst participants with prolonged Tau-ME, those who also had elevated LVEDP, were associated with significantly higher *-dφ'/dV'* (shown in A, >48/≤ 12 vs. >48/>12, P <0.05) and even more prolonged Tau-ME (shown in B, >48/≤ 12 vs. >48/>12, P <0.05). The same was true when subjects were grouped based on alternative LVEDP threshold (≤ or >16 mmHg) (shown in D and E). These results suggest that the rise of *-dφ'/dV'* ultimately reflects a highly impaired early diastolic filling (as measured by exceedingly prolonged Tau-ME), which is accompanied with impaired LV passive compliance (as measured by elevated LVEDP). P-value was obtained using one-way ANOVA with post-hoc Bonferroni's Multiple Comparison test.

Figure S6. Verification of robustness of *-dφ'/dV'* calculation

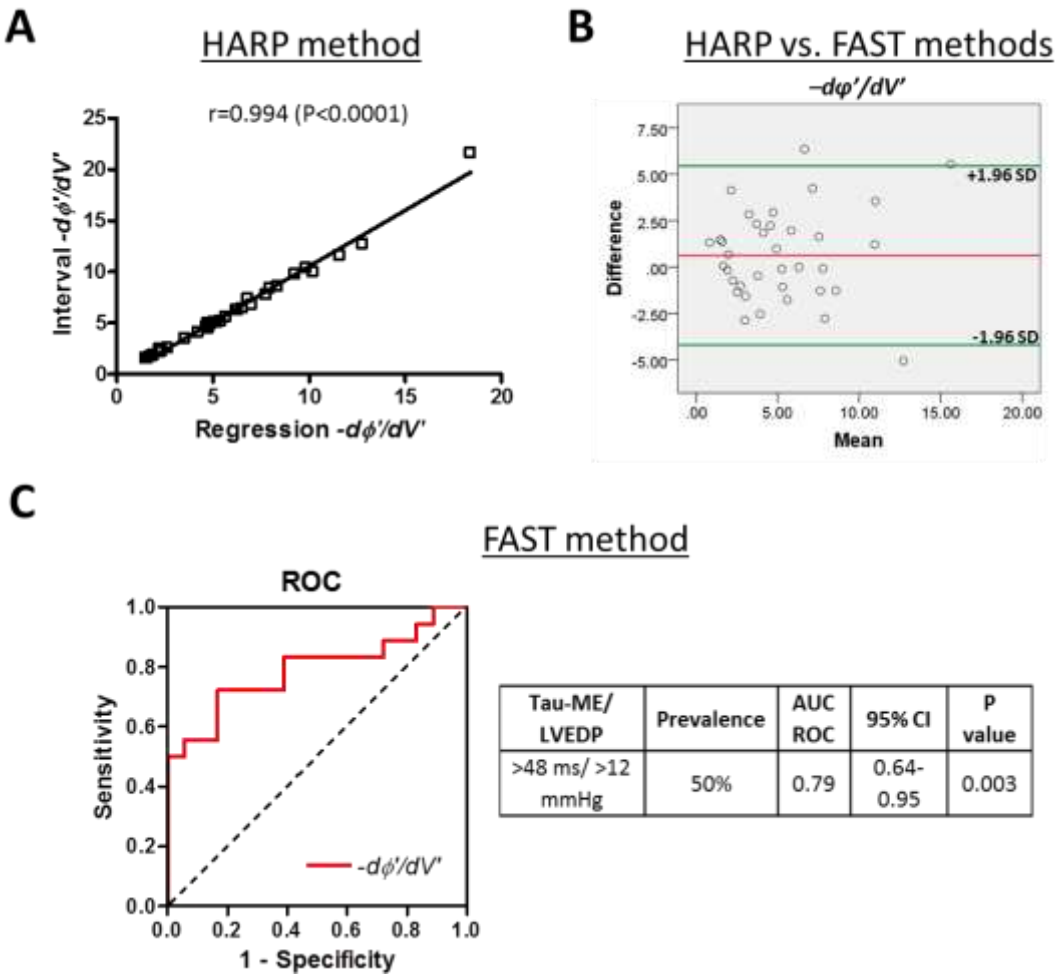

Tau-ME/ LVEDP	Prevalence	AUC ROC	95% CI	P value
>48 ms/ >12 mmHg	50%	0.79	0.64-0.95	0.003

A: Linear regression between interval and regression based calculation of *-dφ'/dV'* values using HARP method. **B:** Bland-Altman plot for values of *-dφ'/dV'* calculated using FAST and HARP methods. **B:** ROC analysis for FAST-method calculated *-dφ'/dV'* to identify LVDD.

Excellent linear correlation between interval and regression HARP based method to calculate *-dφ'/dV'* is observed. When compared with FAST method, the limits of agreement are acceptable. The ROC for FAST based method was similar to HARP based method.